Jul 5th, 12:00 AM - Jul 8th, 12:00 AM

Effect of Boundary-Layer Development on the Water-Surface Fluctuations of Supercritical Flow below a Sluice Gate

Ryugen Satoh
Nihon University, satoh.ryugen@nihon-u.ac.jp

M. Takahashi
Nihon University

I. Ohtsu
Nihon University

Effect of Boundary-Layer Development on the Water-Surface Fluctuations of Supercritical Flow below a Sluice Gate

R. Satoh[1], M. Takahashi[1] and I. Ohtsu[2]
[1]Department of Civil Engineering
Nihon University, College of Science and Technology
Tokyo
JAPAN
[2] Nihon University
Tokyo
JAPAN
E-mail: satou.ryugen@nihon-u.ac.jp

Abstract: *Hydraulic structures with a sluice gate are commonly used for control of the flow. In supercritical flow below a sluice gate, an accurate estimation of the water depth and boundary layer thickness is important for the hydraulic design of a horizontal apron. The relation between water-surface fluctuations and boundary-layer development has not been clarified. The aim of this paper is to experimentally demonstrate the effect of boundary-layer development on water-surface fluctuations of supercritical flow below a sluice gate. It is shown that water surface begins to fluctuate slightly upstream of the critical point. The water-surface fluctuations and turbulence intensities downstream of the critical point are also obtained, which demonstrates the length required for the water-surface fluctuations and turbulence intensity distributions to nearly equal uniform open-channel flow.*

Keywords: *Supercritical flow, boundary-layer development, water-surface fluctuations, turbulence intensity.*

1. INTRODUCTION

Hydraulic structures with a sluice gate are commonly used for control of the flow. For supercritical flow downstream of a sluice gate in a horizontal rectangular channel, the velocity distribution at the section of the vena contracta becomes almost constant (Ohtsu & Yasuda, 1994; Roth & Hager, 1999). A boundary layer develops from the vena contracta section and reaches the water surface. The point where the boundary layer reaches the water surface is known as the critical point. The supercritical flow between the section of the vena contracta and that of the critical point is referred to as the developing flow, as shown in Figure 1.

In the supercritical flow below a sluice gate, an accurate estimation of the water depth and the boundary-layer thickness is important for the hydraulic design of a horizontal apron because the location of the toe of a hydraulic jump is very sensitive to the supercritical flow depth. Recently, Takahashi & Ohtsu (2017; 2009) showed that the boundary-layer development and the water-surface fluctuations at the jump toe have important effects on the characteristics of air entrainment and the velocity fields in hydraulic jumps. Additionally, for a given Froude and Reynolds numbers, Takahashi & Ohtsu (2017) showed that the flow condition for the water surface in the supercritical flow depends on the boundary-layer development. Further study may be required to quantitatively clarify the relation between the water-surface fluctuations and the boundary-layer development of the supercritical flow below a sluice gate.

The aim of this paper is to experimentally demonstrate the effect of the boundary-layer development on the water-surface fluctuations of the supercritical flow below a sluice gate. A method for analytical calculation of the boundary-layer thickness and the supercritical flow depth is examined for the developing flow by using the presented data. Using high-speed video camera images and the measured values of the water-surface fluctuations, it is found that the water-surface fluctuations begin to occur in the developing flow region. The water-surface fluctuations and the turbulence intensities in the section downstream of the critical point are also obtained, determining the region where the distribution of the turbulence intensity is similar to that of uniform open-channel flow.

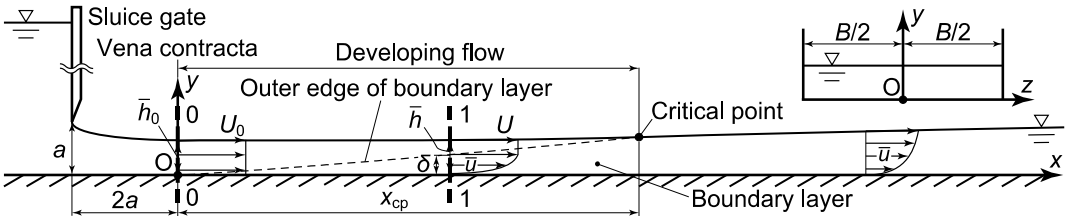

Figure 1 – Definition sketch for a supercritical flow below a sluice gate.

2. EXPERIMENTS AND EXPERIMENTAL SET-UP

The experiments were performed in a horizontal rectangular channel with channel width B = 0.40 m under Fr_0 = 8.0 and Re = 7.2×10^4, where Fr_0 [= $U_0/(g\bar{h}_0)^{1/2}$] is the Froude number at the vena contracta section (section 0 in Figure 1), U_0 is the depth-averaged velocity at section 0, g is the acceleration due to gravity, $\bar{h}_0$ is the time-averaged depth at section 0, Re (= $\rho q/\mu$) is the Reynolds number, ρ is the water density, q is the water discharge per unit width, and μ is the dynamic water viscosity. The water was pumped from a basin to a constant head tank. The water discharge was controlled with a valve and that was measured with an accuracy of ±2% using a sharp-edged weir. The supercritical flow depth was controlled by a sluice gate which composed of a 4 mm thick stainless-steel plate with a sharp lower edge.

The instantaneous water depth h (= $\bar{h} + h'$) and the water-surface fluctuation $(\overline{h'^2})^{1/2}$ were obtained by using an ultrasonic water-level sensor (U.L.S.) of ±1% accuracy with a sampling frequency of 100 Hz and a sampling time of 200 s, where $\bar{h}$ is the time-averaged depth and h' is the fluctuating depth. This measurement was conducted 10 times for each section. It was confirmed that the values of the time-averaged depth determined by using the U.L.S. were equal to those obtained by using a point gauge with a reading accuracy of ±0.1 mm. Additionally, the experiments undertaken confirmed that the vena contracta section is located at a distance 2a downstream the sluice gate (Rajaratnam, 1977; Ohtsu & Yasuda, 1994; Roth & Hager, 1999; Castro-Orgaz & Hager, 2014) and $\bar{h}_0$ = 0.64a (Rajaratnam, 1977; Ohtsu & Yasuda, 1994), where a is the gate opening. The flow conditions for the water-surface fluctuations were observed using a high-speed video camera recording at 1000 fps. To determine the velocity characteristics, the instantaneous velocity u (= $\bar{u} + u'$) was measured by using a one-dimensional laser Doppler velocimeter (L.D.V.), where $\bar{u}$ is the time-averaged velocity in the x-direction, u' is the fluctuating velocity in the x-direction, and x is the horizontal coordinate from the vena contracta. Data were collected at a frequency of up to 4 kHz for each point. The Doppler signals were processed with a sampling frequency of 25 Hz and a sampling time of 164 s. These measurements were carried out along the centerline of the channel (z = 0), where z is the coordinate of a cross section.

3. ANALYSIS OF WATER DEPTH AND BOUNDARY-LAYER THICKNESS

3.1. Developing flow

To show the methods used for analytical calculations of the time-averaged depth and the boundary-layer thickness, it is assumed that the flow is two dimensional and that the loss of energy outside the boundary layer is negligible. Bernoulli's equation for the streamline along the water surface between the vena contracta section (section 0 in Figure 1, x = 0) and the section of the developing flow region (section 1 in Figure 1, $x = x$) is expressed as

$$\frac{U_0^2}{2g} + \bar{h}_0 = \frac{U^2}{2g} + \bar{h} \qquad (1)$$

where U is the velocity outside the boundary layer in the developing flow region. Using the dimensionless quantity J (= U_0/U), Eq. (1) can be written as (Ohtsu & Yasuda, 1994)

$$\frac{\bar{h}}{\bar{h}_0} = \frac{1}{2} Fr_0^2 \left(1 - J^{-2}\right) + 1. \tag{2}$$

The continuity equation between sections 0 and 1 is written as

$$U_0 \bar{h}_0 = U\left(\bar{h} - \delta_1\right) \tag{3}$$

where δ_1 is the displacement thickness, defined as

$$\delta_1 = \int_0^{\bar{h}} \left(1 - \frac{\bar{u}}{U}\right) \mathrm{d}y \tag{4}$$

where y is the vertical coordinate from the channel bed. If the velocity distribution for $\bar{u}$ in the boundary layer is approximated by a one-seventh power law, the relative velocity $\bar{u}/U$ can be expressed as

$$\bar{u}/U = (y/\delta)^{1/7} \quad \text{for} \quad 0 \le y \le \delta \tag{5}$$

where δ is the thickness of the boundary layer, and the velocity distribution $\bar{u}/U$ outside the boundary layer is constant:

$$\bar{u}/U = 1 \quad \text{for} \quad \delta \le y \le \bar{h}\,. \tag{6}$$

Using Eqs. (5) and (6), the displacement thickness δ_1 is written as

$$\delta_1 = \delta/8\,. \tag{7}$$

Or, equivalently,

$$\delta = 8\delta_1. \tag{8}$$

Substituting Eqs. (2) and (7) into Eq. (3), the relative boundary-layer thickness is expressed as (Ohtsu & Yasuda, 1994)

$$\frac{\delta}{\bar{h}_0} = 8\left[\frac{1}{2} Fr_0^2 \left(1 - J^{-2}\right) + 1 - J\right]. \tag{9}$$

For the boundary layer in the open-channel flow, the momentum integral equation for two-dimensional flow can be expressed as

$$\frac{\mathrm{d}\delta_2}{\mathrm{d}x} + \frac{2\delta_2 + \delta_1}{U}\frac{\mathrm{d}U}{\mathrm{d}x} = \frac{C_\mathrm{f}}{2} \tag{10}$$

where δ_2 [$= \int_0^{\bar{h}} (1 - \bar{u}/U)(\bar{u}/U)\,\mathrm{d}y$] is the momentum thickness, C_f [$= \tau_0/(\rho U^2/2)$] is the local skin friction coefficient, and τ_0 is the shear stress on the channel bed. Using Eqs. (5) and (6), the momentum thickness δ_2 is written as

$$\delta_2 = 7\delta/72\,. \tag{11}$$

Substituting Eqs. (7), (9), and (11) into Eq. (10), the following equation is obtained as

$$\mathrm{d}x = \frac{2}{9C_\mathrm{f}}\left[-\frac{37U}{2g} + \frac{23}{U}\left(\frac{U_0^2}{2\mathrm{g}} + \bar{h}_0\right) - \frac{16U_0\bar{h}_0}{U^2}\right]\mathrm{d}U\,. \tag{12}$$

The local skin friction coefficient C_f may be expressed as that for a turbulent boundary layer along a smooth flat plate with a zero pressure gradient (Schlichting, 1979):

$$C_\mathrm{f} = 0.0592(\rho U x/\mu)^{-1/5} \quad \text{for} \quad 3 \times 10^5 \le \rho U x/\mu \le 1 \times 10^7. \tag{13}$$

After substituting Eq. (13) into Eq. (12) and integrating this with respect to x under the condition of the vena contracta section ($U = U_0$ at $x = 0$), the relative distance $x/\bar{h}_0$ is expressed as (Ohtsu & Yasuda, 1994)

$$\frac{x}{\bar{h}_0} = 194Re^{1/4}\left[\frac{37}{99}Fr_0{}^2\left(1 - J^{-11/5}\right) + \frac{23}{9}\left(2 + Fr_0{}^2\right)\left(J^{-1/5} - 1\right) - \frac{8}{9}\left(1 - J^{4/5}\right)\right]^{5/4}. \qquad (14)$$

Thus, for a given Fr_0 and Re, the water-surface profile of the developing flow is calculated by using Eqs. (2) and (14), and the boundary-layer development is calculated by using Eqs. (9) and (14). Furthermore, the value of the critical point x_{cp} is determined by using Eqs. (2), (9), and (14) under the condition at the critical point ($\bar{h}/\bar{h}_0 = \delta/\bar{h}_0$) for a given Fr_0 and Re.

3.2. Supercritical flow downstream of the critical point

In the section downstream of the critical point, the gradually varied flow equation in a horizontal rectangular channel is expressed as

$$\frac{d\bar{h}}{dx} = \left(-\frac{f}{4}\frac{1}{R}\frac{V^2}{2g}\right)\Big/\left(1 - \frac{\alpha BQ^2}{gA^3}\right) \qquad (15)$$

where f is the skin friction coefficient, R is the hydraulic radius, V is the depth-averaged velocity, Q is the discharge, A is the cross-sectional area, and α $\left[= \int_0^{\bar{h}} (\bar{u}/V)^3 \, dy/\bar{h}\right]$ is the energy coefficient. For a smooth rectangular channel, the skin friction coefficient f can be presented as (Knight *et al*., 1984)

$$1/\sqrt{f} = 1.81 \log\left[(4\rho VR/\mu)\sqrt{f}\right] - 0.35 \quad \text{for} \quad 5.3 \times 10^3 \le \rho VR/\mu \le 1.9 \times 10^5. \qquad (16)$$

If $R = \bar{h}$, Eq. (16) can be represented as

$$1/\sqrt{f} = 1.81 \log\left(4Re\sqrt{f}\right) - 0.35. \qquad (17)$$

After substituting $R = \bar{h}$ into Eq. (15), assuming $\alpha = 1$, and integrating this with respect to x under the condition at the section of the critical point ($\bar{h} = \bar{h}_{cp}$ at $x = x_{cp}$) gives (Ohtsu & Yasuda, 1994)

$$\frac{x}{\bar{h}_0} = \frac{8}{f Fr_0{}^2}\left[Fr_0{}^2\left(\frac{\bar{h}}{\bar{h}_0} - \frac{\bar{h}_{cp}}{\bar{h}_0}\right) + \frac{1}{4}\left(\frac{\bar{h}_{cp}}{\bar{h}_0}\right)^4 - \frac{1}{4}\left(\frac{\bar{h}}{\bar{h}_0}\right)^4\right] + \frac{x_{cp}}{\bar{h}_0} \qquad (18)$$

where $\bar{h}_{cp}$ is $\bar{h}$ at the section of the critical point. For a given Fr_0, Re, and $x/\bar{h}_0$, the water-surface profile downstream of the critical point is calculated by using Eqs. (17) and (18). In Eq. (18), the relative value of $\bar{h}_{cp}/\bar{h}_0$ and that of $x_{cp}/\bar{h}_0$ can be obtained from Eqs. (2), (9), and (14) as noted in Section 3.1.

4. RESULTS

4.1. Velocity distributions

For a given Fr_0 and Re, Figure 2(a) shows the velocity distributions for the developing flow, and the solid line in Figure 2(a) illustrates the calculated values obtained with Eq. (5). In the present study, the boundary-layer thickness δ is determined by substituting the displacement thickness δ_1 into Eq. (8). As shown in Figure 2(a), in the range of $0 \le y/\delta \le 1$, the velocity distributions in the boundary layer of the developing flow can be approximated by a one-seventh power law. For the outside of the boundary layer ($y/\delta \ge 1$), the values of the relative velocity $\bar{u}/U$ become constant ($\bar{u}/U = 1$). Additionally, the effects of

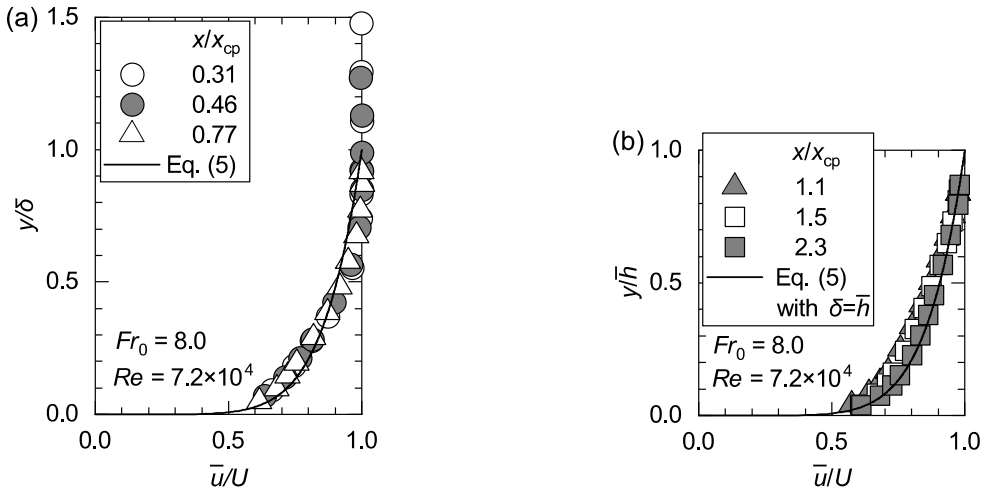

Figure 2 – Velocity distributions for (a) the developing flow; (b) a section downstream of the critical point.

the relative distance x/x_{cp} on the velocity distribution of the developing flow are negligible. Figure 2(b) shows the velocity distributions in the section downstream of the critical point, and the solid line in Figure 2(b) illustrates the calculated values obtained by using Eq. (5) with $\delta = \bar{h}$. The relative velocity distributions in the section downstream of the critical point are approximated by a one-seventh power law, and the effects of x/x_{cp} on the relative velocity distribution are negligible.

4.2. Water-surface profile and boundary-layer development

The water-surface profile and the boundary-layer development in accordance with $\bar{h}/\bar{h}_0 = f(x/x_{cp})$ and $\delta/\bar{h}_0 = f(x/x_{cp})$ are presented in Figure 3 under a given Fr_0 and Re. The dashed line in Figure 3 shows the values of the boundary-layer thickness calculated using Eqs. (9) and (14). The solid line in Figure 3 shows the values of the water depth for the developing flow calculated using Eqs. (2) and (14), and the dotted-dashed line in Figure 3 shows the values of the water depth for the section downstream of the critical point calculated using Eqs. (17) and (18). As shown in Figure 3, in the developing flow ($0 < x/x_{cp} < 1$), the boundary-layer thickness $\delta/\bar{h}_0$ and the time-averaged depth $\bar{h}/\bar{h}_0$ increase with the relative distance x/x_{cp}. At the critical point ($x/x_{cp} = 1$), the boundary-layer thickness is equal to the time-averaged depth. In the section downstream of the critical point ($x/x_{cp} > 1$), $\bar{h}/\bar{h}_0$ increases with the relative distance x/x_{cp}. Additionally, the calculated values of the water depth $\bar{h}/\bar{h}_0$ and the boundary-layer thickness $\delta/\bar{h}_0$ are in agreement with the experimental values of $\bar{h}/\bar{h}_0$ and $\delta/\bar{h}_0$, respectively.

4.3. Turbulence intensity distributions

For a given Fr_0 and Re, the turbulence intensity distributions for the developing flow ($0 < x/x_{cp} < 1$) in accordance with $(\overline{u'^2})^{1/2}/U = f(y/\delta)$ are shown in Figure 4(a). In the boundary layer ($0 < y/\delta \lesssim 1$), as shown in Figure 4(a), the values of the turbulence intensity $(\overline{u'^2})^{1/2}/U$ become small with increasing the relative height y/δ. Outside the boundary layer for $y/\delta \gtrsim 1.2$, the values of $(\overline{u'^2})^{1/2}/U$ are smaller than those in the boundary layer, and the values of $(\overline{u'^2})^{1/2}/U$ outside the boundary layer are nearly constant. Klebanoff (1955) indicated that the instantaneous position of the edge of the turbulent boundary layer has a random character, and the edge rarely extends outside the region of $0.4 \le y/\delta \le 1.2$. This discussion means that the fully turbulent region and the intermittent region are formed in $y/\delta < 0.4$ and $0.4 \le y/\delta \le 1.2$, respectively. Therefore, in the supercritical flow below a sluice gate, it may be considered that the region in $0.4 \le y/\delta \le 1.2$ is intermittently turbulent.

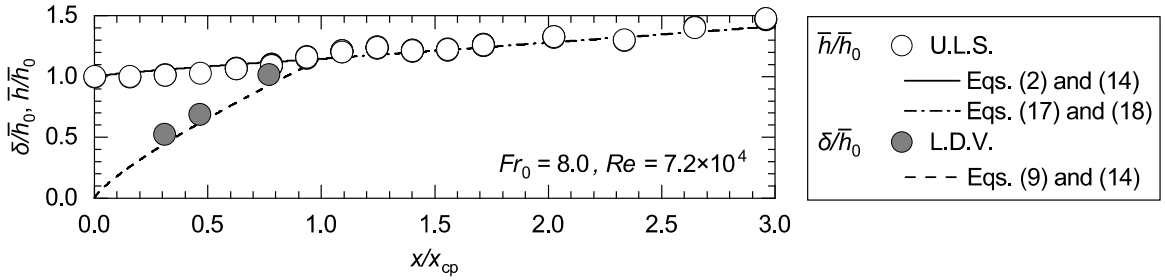

Figure 3 – Water-surface profile and boundary-layer development.

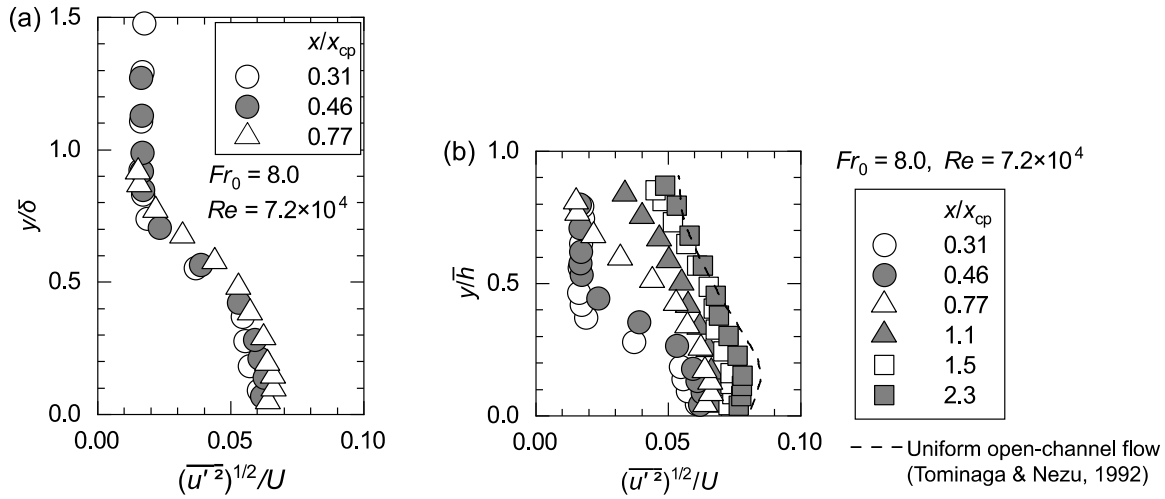

Figure 4 – Turbulence intensity distributions for (a) the variation of y/δ with $(\overline{u'^2})^{1/2}/U$; (b) the variation of $y/\bar{h}$ with $(\overline{u'^2})^{1/2}/U$.

For a given Fr_0 and Re, Figure 4(b) shows the variation of the turbulence intensity $(\overline{u'^2})^{1/2}/U$ with the relative height $y/\bar{h}$ in the supercritical flow below a sluice gate. In Figure 4(b), the dashed line is the distribution of the turbulence intensity for uniform open-channel flow (Tominaga & Nezu, 1992). In the range of $0 < x/x_{cp} \lesssim 0.8$, as shown in Figure 4(b), the measured values of $(\overline{u'^2})^{1/2}/U$ near the water surface ($y/\bar{h} \approx 1$) are small and independent of the relative distance x/x_{cp}. In the range of $1 < x/x_{cp} \lesssim 1.5$, the measured values of $(\overline{u'^2})^{1/2}/U$ near the water surface ($y/\bar{h} \approx 1$) increase with the relative distance x/x_{cp}. In the range of $x/x_{cp} \gtrsim 1.5$, the magnitude and distribution of the turbulence intensity is independent of x/x_{cp}. It is shown that the distributions for the turbulence intensity in the range of $x/x_{cp} \gtrsim 1.5$ are nearly equal to those in the uniform open-channel flow, as shown by the dashed line in Figure 4(b). Therefore, in the supercritical flow below a sluice gate, it is considered that the fully developed flow is formed in the range of $x/x_{cp} \gtrsim 1.5$.

4.4. Water-surface fluctuations

The high-speed video camera images for the water-surface fluctuations for a given Fr_0 and Re are shown in Figure 5. In Figure 5, the values of x/x_{cp} and those of the boundary-layer development $\delta/\bar{h}$ are calculated by using Eqs. (2), (9), and (14). As shown in Figure 5(a), the water surface in the range of $0 \le x/x_{cp} \lesssim 0.2$ ($0 \le \delta/\bar{h} \lesssim 0.3$) is smooth like transparent glass. This is because the turbulence in the boundary layer does not reach the water surface. As shown in Figure 5(b), the water surface begins to fluctuate slightly in the range of $0.6 \lesssim x/x_{cp} \lesssim 0.8$ ($0.7 \lesssim \delta/\bar{h} \lesssim 0.8$). This result might show that the boundary layer reaches the water surface intermittently in the range of $0.6 \lesssim x/x_{cp} \lesssim 0.8$ ($0.7 \lesssim \delta/\bar{h} \lesssim 0.8$). As shown in Figure 5(c), the water-surface fluctuations at the critical point (x/x_{cp} =1) are large compared with Figures 5(a) and 5(b). As shown in Figure 5(d), the water-surface fluctuations in the range of $1.6 \lesssim x/x_{cp} \lesssim 1.7$ are larger than those shown in Figures 5(a), 5(b), and 5(c).

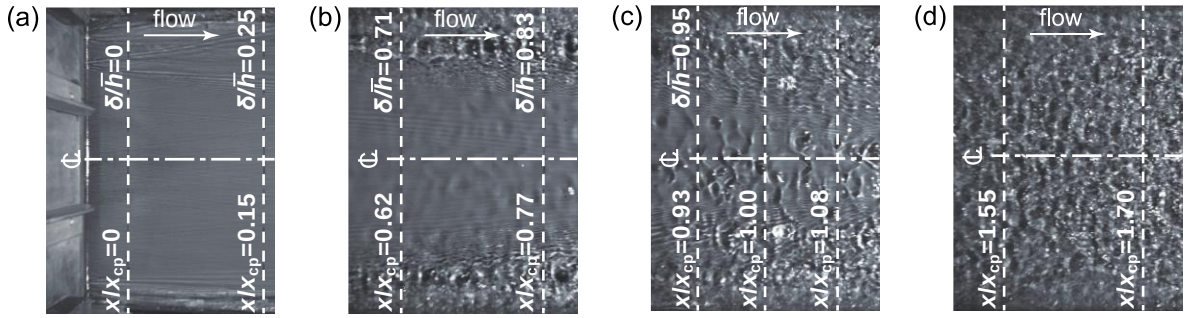

Figure 5 – Flow condition of water-surface fluctuations with Fr_0 = 8.0 and Re = 7.2×10^4 for (a) 0 ≤ x/x_{cp} ≲ 0.2; (b) 0.6 ≲ x/x_{cp} ≲ 0.8; (c) 0.9 ≲ x/x_{cp} ≲ 1.1; (d) 1.6 ≲ x/x_{cp} ≲ 1.7.

For a given Fr_0 and Re, Figure 6 shows the relation between the water-surface fluctuations $(\overline{h'^2})^{1/2}/\bar{h}$ and the boundary-layer development $\delta/\bar{h}$ in the developing flow region, and the values of $\delta/\bar{h}$ are calculated by using Eqs. (2), (9), and (14). The dashed line in Figure 6 indicates the trend for the water-surface fluctuations with boundary-layer development $\delta/\bar{h}$. As shown in Figure 6, the measured values of $(\overline{h'^2})^{1/2}/\bar{h}$ in the range of 0 ≤ $\delta/\bar{h}$ ≲ 0.6 are small. However, the measured values of $(\overline{h'^2})^{1/2}/\bar{h}$ in the range of 0.7 ≲ $\delta/\bar{h}$ ≲ 1.0 increase with $\delta/\bar{h}$, illustrating that water-surface fluctuations may begin to occur if 0.7 ≲ $\delta/\bar{h}$ ≲ 0.8. This is because the water surface begins to fluctuate slightly in the range of 0.7 ≲ $\delta/\bar{h}$ ≲ 0.8 (0.6 ≲ x/x_{cp} ≲ 0.8), as shown in Figure 5(b). It may be similar to air flow on a flat plate in the turbulent boundary layer intermittently reaching y/δ = 1.2 (Klebanoff, 1955).

Figure 7 shows the streamwise change of water-surface fluctuations in the supercritical flow below a sluice gate for a given Fr_0 = 8.0 and Re = 7.2×10^4. The dashed line in Figure 7 indicates the trend for the water-surface fluctuations with the relative distance x/x_{cp}. The values of the water-surface fluctuations $(\overline{h'^2})^{1/2}/\bar{h}$ in the range of 0 ≤ x/x_{cp} ≲ 0.5 are small, and these results correspond with Figure 5(a). The values of $(\overline{h'^2})^{1/2}/\bar{h}$ in the range of 0.5 ≲ x/x_{cp} ≲ 1.5 increase with the relative distance x/x_{cp}. The water surface, as shown in Figures 5(b) and 5(c), changes from smooth to uneven in the range of 0.5 ≲ x/x_{cp} ≲ 1.5. Whereas, as shown in Figure 7, the values of $(\overline{h'^2})^{1/2}/\bar{h}$ in the range of x/x_{cp} ≳ 1.5 are nearly constant, and the values of $(\overline{h'^2})^{1/2}/\bar{h}$ in the range of x/x_{cp} ≳ 1.5 are larger than those in the range of 0 ≤ x/x_{cp} < 1.5. These results might demonstrate that the water-surface fluctuations in the range of x/x_{cp} ≳ 1.5 are similar to those obtained for uniform open-channel flow because the distributions of the turbulence intensity in x/x_{cp} ≳ 1.5 are nearly equal to those in uniform open-channel flow, as noted in Section 4.3. Therefore, it is considered that the water-surface fluctuations

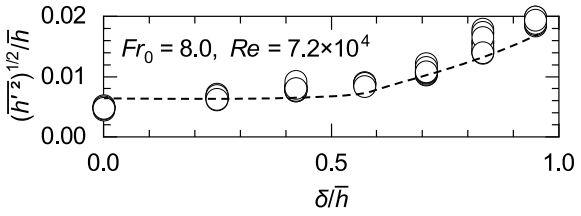

Figure 6 – Relation between water-surface fluctuations and boundary-layer development.

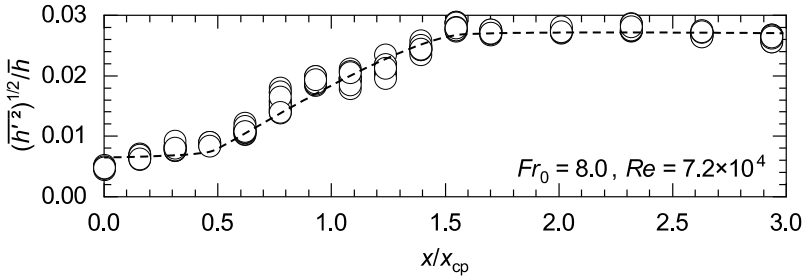

Figure 7 – Streamwise change of water-surface fluctuations.

in the range of $x/x_{cp} \gtrsim 1.5$ are fully developed for Fr_0 = 8.0 and Re = 7.2×10^4. To clarify the water-surface fluctuations of the supercritical flow below a sluice gate, further measurements for a wide range of Fr_0 and Re are needed.

5. CONCLUSIONS

The effect of the boundary-layer development on the water-surface fluctuations of the supercritical flow below a sluice gate in a horizontal rectangular channel was experimentally demonstrated for Fr_0 = 8.0 and Re = 7.2×10^4. The results in this paper are summarized as follows:

(i) The time-averaged velocity distributions in the boundary layer for the developing flow and a section downstream of the critical point can be approximated by a one-seventh power law.

(ii) For a given Fr_0 and Re, the water-surface profile and the boundary-layer development in the developing flow region can be calculated by using Eqs. (2), (9), and (14). The water-surface profile downstream of the critical point is obtained by using Eqs. (17) and (18).

(iii) In the developing flow region, high-speed video camera images show that the water-surface fluctuations begin to occur if the boundary-layer development $\delta/\bar{h}$ becomes equal to 0.7–0.8.

(iv) The water-surface fluctuations and the turbulence intensities in a section downstream of the critical point are nearly equal to those in uniform open-channel flow if the relative distance x/x_{cp} is greater than 1.5.

6. ACKNOWLEDGEMENTS

The second author was financially supported by the Japan Society for the Promotion of Science (JSPS), Grant Number 19K04624.

7. REFERENCES

Castro-Orgaz, O. and Hager, W.H. (2014), *Transitional flow at standard sluice gate*, Journal of Hydraulic Research, IAHR, 52 (2), 264–273.

Klebanoff, P.S. (1955), Characteristics of turbulence in a boundary layer with zero pressure gradient, NACA Technical Report 1247, National Advisory Committee for Aeronautics, Hampton, NASA-Langley Research Center.

Knight, D.W., Demetriou, J.D. and Hamed, M.E. (1984), *Boundary shear in smooth rectangular channels*, Journal of Hydraulic Engineering, ASCE, 110 (4), 405–422.

Ohtsu, I. and Yasuda, Y. (1994), *Characteristics of supercritical flow below sluice gate*, Journal of Hydraulic Engineering, ASCE, 120 (3), 332–346.

Rajaratnam, N. (1977), *Free flow immediately below sluice gates*, Journal of the Hydraulics Division, ASCE, 103 (4), 345–351.

Roth, A. and Hager, W.H. (1999), *Underflow of standard sluice gate*, Experiments in Fluids, Springer, 27, 339–350.

Schlichting, H. (1979), *Boundary-layer theory*, seventh edition, McGraw-Hill, New York.

Takahashi, M. and Ohtsu, I. (2009), *Effect of inflow condition on air entrainment characteristics in hydraulic jump*, *Proceedings of the 33rd IAHR congress*, Vancouver, BC, Canada, 4917–4924.

Takahashi, M. and Ohtsu, I. (2017), *Effects of inflows on air entrainment in hydraulic jumps below a gate*, Journal of Hydraulic Research, IAHR, 55 (2), 259–268.

Tominaga, A. and Nezu, I. (1992), *Velocity profiles in steep open-channel flows*, Journal of Hydraulic Engineering, ASCE, 118 (1), 73–90.